Journal of
Applied Crystallography
ISSN 0021-8898
Editor: **Anke R. Pyzalla**

The crystal structure of perdeuterated methanol hemiammoniate ($CD_3OD{\cdot}0.5ND_3$) determined from neutron powder diffraction data at 4.2 and 180 K

A. D. Fortes, I. G. Wood and K. S. Knight

J. Appl. Cryst. (2010). **43**, 328–336

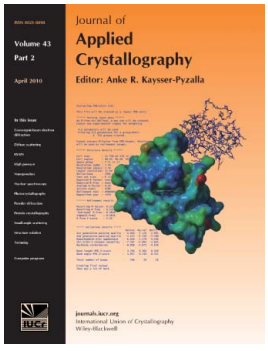

Journal of
Applied Crystallography
ISSN 0021-8898

Received 1 October 2009
Accepted 10 February 2010

The crystal structure of perdeuterated methanol hemiammoniate ($CD_3OD{\cdot}0.5ND_3$) determined from neutron powder diffraction data at 4.2 and 180 K

A. D. Fortes,[a,b]* I. G. Wood[a,b] and K. S. Knight[c,d]

[a]Department of Earth Sciences, University College London, Gower Street, London WC1E 6BT, UK, [b]Centre for Planetary Sciences at University College London/Birkbeck, Gower Street, London WC1E 6BT, UK, [c]ISIS Facility, STFC Rutherford Appleton Laboratory, Harwell Science and Innovation Campus, Chilton, Didcot, Oxfordshire OX11 0QX, UK, and [d]The Natural History Museum, Cromwell Road, London SW7 5BD, UK. Correspondence e-mail: andrew.fortes@ucl.ac.uk

The crystal structure of perdeuterated methanol hemiammoniate, $CD_3OD{\cdot}{\cdot}0.5ND_3$, has been solved from neutron powder diffraction data collected at 4.2 and 180 K. The structure is orthorhombic, space group $Pn2_1a$ ($Z = 4$), with unit-cell dimensions a = 12.70615 (16), b = 8.84589 (9), c = 4.73876 (4) Å, V = 532.623 (8) Å^3 [ρ_{calc} = 1149.57 (2) kg m^{-3}] at 4.2 K, and a = 12.90413 (16), b = 8.96975 (8), c = 4.79198 (4) Å, V = 554.656 (7) Å^3 [ρ_{calc} = 1103.90 (1) kg m^{-3}] at 180 K. The crystal structure was determined by *ab initio* methods from the powder data; atomic coordinates and isotropic displacement parameters were subsequently refined by the Rietveld method to $R_p \simeq 2\%$ at both temperatures. The crystal structure comprises a three-dimensionally hydrogen-bonded network in which the ND_3 molecules are tetrahedrally coordinated by the hydroxy moieties of the methanol molecule. This connectivity leads to the formation of zigzag chains of ammonia–hydroxy groups extending along the c axis, formed *via* N—D···O hydrogen bonds; these chains are cross-linked along the a axis through the hydroxy moiety of the second methanol molecule *via* N—D···O and O—D···O hydrogen bonds. This 'bridging' hydroxy group in turn donates an O—D···N hydrogen bond to ammonia in adjacent chains stacked along the b axis. The methyl deuterons in methanol hemiammoniate, unlike those in methanol monoammoniate, do not participate in hydrogen bonding and reveal evidence of orientational disorder at 180 K. The relative volume change on warming from 4.2 to 180 K, $\Delta V/V$, is + 4.14%, which is comparable to, but more nearly isotropic (as determined from the relative change in axial lengths, *e.g.* $\Delta a/a$) than, that observed in deuterated methanol monohydrate, and very similar to what is observed in methanol monoammoniate.

1. Introduction

The ammonia–methanol system presents an interesting counterpoint to the water–methanol system; the latter is of great importance in biological and industrial chemistry, and this system has been the subject of many experimental and computational studies. In contrast, very little study has been devoted to the ammonia–methanol system. A 1:1 complex of CH_3OH and NH_3 was identified in the gas phase by Millen & Zabicky (1962, 1965). This complex was subsequently studied experimentally using infrared spectroscopy (Hussein & Millen, 1974) and microwave spectroscopy (Fraser *et al.*, 1988). The 1:1 methanol–ammonia complex has also been studied computationally using classical potentials (Brink & Glasser, 1982) and quantum mechanical methods (Li *et al.*, 1997). Vapour–liquid equilibria in the ammonia–methanol system were measured by Inomata *et al.* (1988), Feng *et al.* (1999) and Schäfer *et al.* (2007), and the viscosity of the liquid was measured by Frank *et al.* (1996). The only known study of liquid–solid phase relations in the ammonia–methanol system is that of Kargel (1990, 1992), shown in Fig. 1. Kargel identified two solid compounds; these are methanol monoammoniate ($CH_3OH{\cdot}NH_3$), which melts congruently at 218.0 K, and methanol hemiammoniate ($CH_3OH{\cdot}0.5NH_3$), which melts incongruently at 194.6 K. Kanesaka & Kawai (1982) and Kanesaka *et al.* (1984) had earlier collected infrared spectra from frozen mixtures with a range of ammonia-to-methanol ratios at 77 K; this work did not identify whether the specimens were crystalline or amorphous, although the authors observed that the spectra did not change upon annealing.

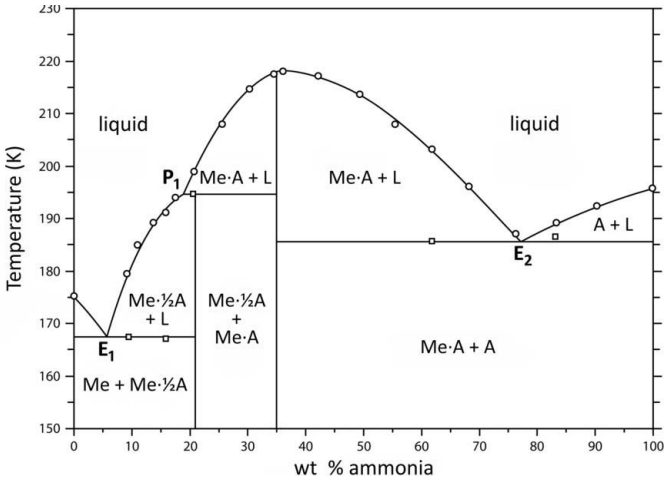

Figure 1
The protonated ammonia–methanol system, reproduced with permission from Kargel (1992), based on original data (open circles) from Kargel (1990). Me = methanol, A = ammonia, Me·½A = methanol hemiammoniate and Me·A = methanol monoammoniate. Eutectics $\mathbf{E_1}$ and $\mathbf{E_2}$ are at 167.2 K, 5.7 wt% NH_3 and 185.6 K, 77.3 wt% NH_3, and peritectic $\mathbf{P_1}$ is at 194.6 K, 19.0 wt% NH_3.

Although this binary system has received almost no attention, the interaction between ammonia and methanol, in both the liquid and the solid state, provides a very simple archetypal system for understanding hydrogen bonding, particularly weak hydrogen bonds which may be donated by the methyl group, the latter having been the subject of long-standing debate (*e.g.* Steiner & Desiraju, 1998: Yukhnevich & Tarakanova, 1998). In an earlier structural analysis of methanol monohydrate (Fortes, 2006), it was discovered that the water molecules and hydroxy moieties of the methanol molecule participate in strong hydrogen bonds, forming a two-dimensional sheet-like structure. This sheet is decorated on its upper and lower surfaces by the hydrophobic methyl moiety of the methanol molecule; adjacent sheets are not hydrogen bonded, but interact only by weak van der Waals forces. This results in a very large volume thermal expansion coefficient, 527×10^{-6} K^{-1} at 160 K, the majority of which is due to interlayer expansion perpendicular to the strongly bonded sheets (Fortes *et al.*, 2007). Noting that the methanol ammoniates have melting points equal to or greater than any other solid in the ternary water–ammonia–methanol system (*cf.* Kargel, 1992), with the exception of water–ice, we had speculated that the methanol ammoniates have a relatively strong three-dimensional hydrogen-bond network rather than the two-dimensional network found in $CH_3OH{\cdot}H_2O$. There are few examples of cryocrystals that are structurally dominated by ammonia; the closest analogue to the mono- and hemiammoniates may be ammonia hemihydrate, which is a fully three-dimensional hydrogen-bonded crystal (Loveday & Nelmes, 2000).

Lastly, both methanol and ammonia have been detected in the solid phase in interstellar and cometary ices, and may also be an important constituent of cryovolcanic liquids on the icy bodies in the outer solar system (Kargel, 1992; Lopes *et al.*, 2007). Hence, methanol ammoniates could be accessory mineral phases in a variety of extraterrestrial environments. Characterization of the crystal structures of these compounds is relevant to possible future *in situ* measurements of icy satellite mineralogy (*e.g.* Fortes, Wood, Dobson & Fewster, 2009) and to characterization of phases observed in the course of future laboratory measurements upon the ternary system.

We have collected neutron powder diffraction data from perdeuterated specimens of methanol monoammoniate and methanol hemiammoniate, with the objective of determining their crystal structures. The structure of neither ammoniate was known previously; in contrast to the monohydrate, there have been no prior X-ray studies to indicate the symmetry or unit-cell dimensions. Our solution of the methanol monoammoniate crystal structure is presented elsewhere (Fortes, Wood & Knight, 2009); the present paper reports our results for methanol hemiammoniate.

The work described here was carried out on the High Resolution Powder Diffractometer, HRPD (Ibberson *et al.*, 1992), at the STFC ISIS neutron spallation source, Rutherford Appleton Laboratory, UK, which has the best combination of resolution and flux of any similar instrument in the world. Given the large incoherent scattering length of the H atom, a perdeuterated analogue, $CD_3OD{\cdot}0.5ND_3$, was used in order to achieve good signal-to-noise in the measured diffraction data (*cf.* Finney, 1995).

2. Experimental

2.1. Sample preparation and data collection

An evacuated glass bulb immersed in an acetone bath cooled to 210 K with dry ice was used to condense liquid deuterated ammonia (Aldrich Chemical Co., 99 at.% D), to which was added the appropriate quantity of deuterated methanol (Aldrich Chemical Co., 99.8 at.% D) necessary to yield a solution of 2:1 molar stoichiometry (78.28 wt% CD_3OD). The 2:1 solution was left immersed in the cold acetone bath for ∼30 min; during this time we observed the growth of small white crystals, which we believe to have been methanol monoammoniate. Although these were melted prior to loading of the sample into the cryostat it is possible that microscopic seed crystals remained. All of the 2:1 solution in the bulb was poured into a stainless steel cryomortar (precooled to liquid nitrogen temperature), forming a toffee-like solid, which became brittle when liquid N_2 (L-N_2) was applied directly; this solid material was ground to a coarse powder very easily. The powdered solid was transferred to a pre-prepared[1] aluminium-framed slab can at L-N_2 temperatures. The back window of the slab can was quickly screwed into place and the centre-stick/slab-can assembly was moved (with the sample immersed in an L-N_2 dewar) to an OC100 Orange cryostat on the HRPD beamline. A brief inspection of the

[1] Before loading, the slab can was screwed to a cryostat centre stick and wired with heating elements and an RhFe resistance thermometer; the front window was screwed into place with a gadolinium/cadmium foil sandwich over the exposed aluminium frame and gadolinium foil shielding around the exposed screw heads. The slab can was held in a shallow plastic dish of liquid nitrogen whilst the powder sample was loaded.

diffraction pattern at ∼100 K revealed Bragg reflections, indicating that the specimen was crystalline. The specimen was warmed to 180 K and data were collected in the 30–130 ms time-of-flight (t-o-f) window for 450.0 μAh, after which data were collected for 115.1 μAh with the choppers re-phased to allow examination of the 100–200 ms t-o-f window. The short t-o-f window permits access to *d*-spacing ranges of 0.66–2.47 Å in HRPD's backscattering detectors (2θ = 168.33°), 0.92–3.45 Å in the 90° detector banks and 2.49–9.26 Å in the low-angle detectors (average 2θ = 30°). In the long t-o-f window, the backscattering and 90° banks, respectively, view *d*-spacing ranges of 2.17–3.93 and 3.03–5.46 Å; no useful data were obtained in the low-angle bank with this flight time window. The temperature of the specimen was then reduced to 4.2 K and data were collected only in the short t-o-f window for 109.6 μAh. The specimen exhibited essentially the same diffraction pattern at 4.2 K as observed at 180 K, albeit with slightly broader Bragg peaks and greatly reduced diffuse scattering at short *d* spacings (compare Figs. 2 and 3).

The diffraction data were normalized to the incident monitor spectrum, corrected for detector efficiency using a vanadium standard and exported as *GSAS*-format (Larsen & Von Dreele, 2000) raw files for analysis.

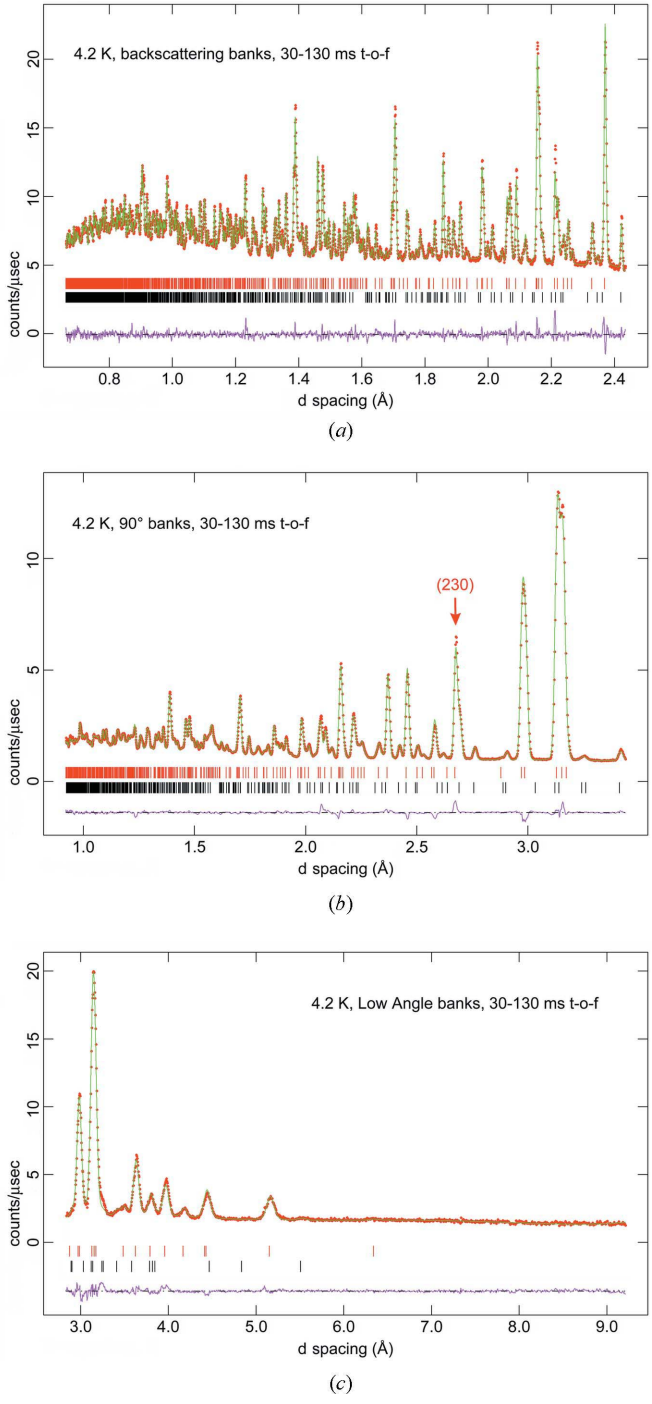

Figure 2
Neutron powder diffraction patterns at 4.2 K using the 30–130 ms t-o-f window in (*a*) the backscattering detectors, (*b*) the 90° banks and (*c*) the low-angle bank. Upper red tick marks show the expected positions of methanol hemiammoniate reflections, and lower black tick marks those of the methanol monoammoniate reflections.

2.2. Indexing and structure solution

It was immediately obvious that the diffraction patterns contained no reflections that could be attributed to either α- or β-methanol (Torrie *et al.*, 1989, 2002), or to cubic solid ammonia (Hewat & Riekel, 1979). However, it became clear – particularly upon inspection of the 100–200 ms backscattering data – that there were reflections from methanol monoammoniate present. Subsequent refinement of the methanol monoammoniate and hemiammoniate phase fractions (described in §2.3) revealed that the specimen contained 17.8 (2) wt% methanol monoammoniate. It is unlikely that methanol was lost from the specimen during preparation, it being far more likely to have lost ammonia, and consequently to have become enriched in methanol. There are then only two remaining possible explanations for the observed phase mixture: the first is that the stoichiometry of the starting

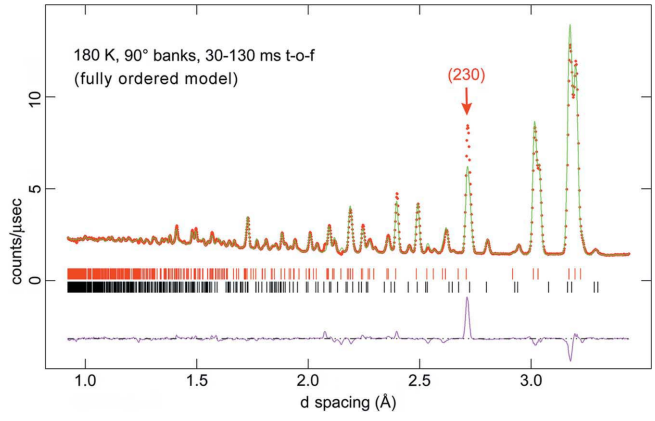

Figure 3
Neutron powder diffraction pattern collected at 180 K in the 90° banks in the 30–130 ms t-o-f window, used to refine the fully ordered model obtained from the 4.2 K refinement. Note the large misfit to the 230 reflection. Compare this figure with panel (*c*) of Fig. 4, which was refined using a model containing disordered methyl deuterons. Upper red tick marks show the expected positions of methanol hemiammoniate reflections, and lower black tick marks those of the methanol monoammoniate reflections.

material was substantially incorrect, which we consider unlikely; the second is that the liquid – despite rapid quenching – experienced partial crystallization, as one would expect from the liquidus boundaries shown in Fig. 1. One can see from Fig. 1 that a liquid with a composition corresponding to methanol hemiammoniate, upon cooling, intersects the liquidus near 200 K (in the protonated system) and begins to crystallize methanol monoammoniate; this continues until the liquid composition is driven to the peritectic $\mathbf{P_1}$. If we accept the accuracy of the phase diagram for the protonated system measured by Kargel (1990, 1992), then at this peritectic point, the system comprises a mixture of ∼13 wt% methanol monoammoniate crystals in liquid of composition $\mathbf{P_1}$. Under equilibrium conditions, liquid $\mathbf{P_1}$ will react with the methanol monoammoniate crystals to form methanol hemiammoniate before cooling can proceed. However, at high cooling rates, this reaction may be inhibited, preserving the methanol monoammoniate crystals, and causing liquid $\mathbf{P_1}$ to freeze into a mixture of methanol hemiammoniate with either solid methanol or methanol-rich glass. We believe that this is the most plausible explanation for the presence of significant quantities of methanol monoammoniate in our sample. It is clear from the phase diagram that only small shifts in the liquidi upon deuteration would be sufficient to yield nearer 18 wt% methanol monoammoniate than 13 wt% at peritectic $\mathbf{P_1}$. Since there is no obvious solid methanol (either α- or β-phase) in the specimen, we must conclude that there is a

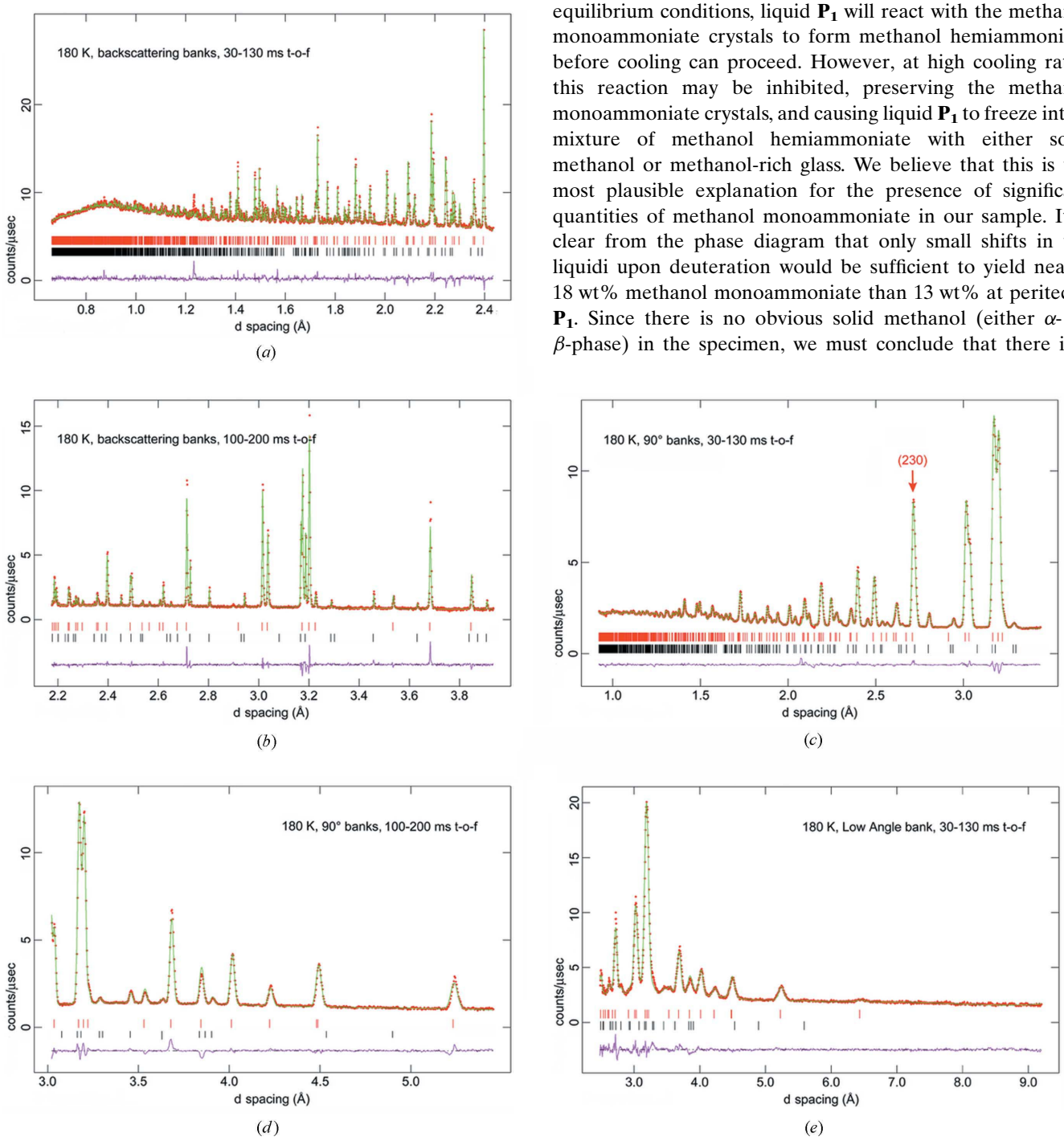

Figure 4
Neutron powder diffraction patterns at 180 K in the backscattering detectors observed in (*a*) the 30–130 ms t-o-f window and (*b*) the 100–200 ms t-o-f window; in the 90° banks observed in (*c*) the 30–130 ms t-o-f window and (*d*) the 100–200 ms t-o-f window; and in the low-angle bank observed in (*e*) the 30–130 ms t-o-f window. In each plot, the refinement reported is the structure with disordered methyl groups described in the text. Compare Fig. 4(*c*) with Fig. 3 to see the improvement in the fit resulting from adoption of the disordered model. Upper red tick marks show the expected positions of methanol hemiammoniate reflections, and lower black tick marks those of the methanol monoammoniate reflections.

small quantity (estimated from the phase diagram to be <8 wt%) of methanol-rich glass present, which will make a contribution to the background structure of the diffraction pattern.

After subtraction of the reflections due to methanol monoammoniate, the 180 K backscattering data collected in the 100–200 ms t-o-f window were indexed using *DICVOL04* (Boultif & Louër, 2004) with an orthorhombic unit cell having dimensions $a = 12.9035\ (9)$, $b = 8.9708\ (5)$, $c = 4.7927\ (2)$ Å, $V = 554.77$ Å^3, the figures of merit being $M(23) = 77.7$ (de Wolff, 1968) and $F(23) = 141.0$ [0.0033, 50] (Smith & Snyder, 1979). Using the molecular volumes of CD_3OD in β-methanol at 170 K (53.63 Å^3; Torrie *et al.*, 2002) and of cubic ND_3 at 180 K (33.65 Å^3; Hewat & Riekel, 1979), we can obtain an estimate of the unit-cell volume as a function of the number of formula units per unit cell. The case of $Z = 4$ yields $V = 563.64$ Å^3, which differs from the indexed unit-cell volume by only 1.6%.

Analysis of the systematic absences narrowed the range of likely space groups to *Pnaa*, *Pnma* and $Pn2_1a$. Of these, only the noncentrosymmetric space group $Pn2_1a$ satisfies the requirement of fourfold general positions. The gross atomic structure was subsequently solved in space group $Pn2_1a$ from the 180 K powder data using the parallel tempering algorithm implemented in *FOX* (Version 1.6.99; Favre-Nicolin & Černý, 2002, 2004). Inputs for the solution process were the backscattering, 90° and low-angle diffraction patterns collected at 180 K in the 30–130 and 100–200 ms t-o-f windows, along with profile coefficients determined by Le Bail fitting to the data with *GSAS*/*Expgui* (Larsen & Von Dreele, 2000; Toby, 2001), background points obtained by spline interpolation in *FOX* and definitions of the molecular fragments in the asymmetric unit in the form of Z matrices. These Z matrices were created using the interatomic distances and angles found in solid α-methanol (Torrie *et al.*, 1989) and cubic ammonia (Hewat & Riekel, 1979); *FOX* was instructed to treat the molecules as rigid bodies. The unit-cell dimensions and atomic coordinates for the accessory methanol monoammoniate were entered explicitly, using the results of the 180 K refinement reported by Fortes, Wood & Knight (2009). One initial test run of three million trials, followed by five sequential runs of one million trials each, were performed, in which the crystal structure and the five diffraction patterns were optimized; these consistently produced near identical structures with chemically sensible molecular arrangements, and the structure with the lowest overall cost function was exported as a CIF to form the basis for Rietveld refinement with *GSAS*.

2.3. Structure refinement

The initial structural model for methanol hemiammoniate produced by *FOX* was used as input for the Rietveld refinement in *GSAS*. For the accessory methanol monoammoniate at 4.2 and 180 K the structural models with anisotropic displacement parameters (Fortes, Wood & Knight, 2009) were fixed, and only the unit-cell dimensions, phase fraction and peak-profile coefficients for this component were varied. Beginning with the refinement of the 4.2 K structure using only the 30–130 ms backscattering data, bond-distance restraints, listed as follows, were applied in the early cycles of refinement with a moderately high weighting: C—O = 1.415 (5) Å; C—D = 1.080 (5) Å; O—D = 0.975 (5) Å; N—D = 1.012 (5) Å; methyl D—D = 1.775 (5) Å; methyl D—O = 2.04 (1) Å; and ammonia D—D = 1.632 (5) Å. From the 4.2 K data set, this model refined to $R_p = 2.13\%$ ($\chi^2 = 9.183$), with freely varied isotropic displacement parameters on each atom, a 15-term Chebyschev polynomial background function, one absorption coefficient and three peak-profile coefficients for each phase. Relaxation of the bond-distance restraints allowed the goodness-of-fit to improve to $R_p = 1.98\%$ ($\chi^2 = 6.865$). Attempts were then made to refine anisotropic displacement parameters, but this consistently resulted in nonpositive definite displacement ellipsoids. Given the large number of structural variables required for such a refinement (minimum of 144; x, y, z + U_{ij} for 16 atoms), and the presence of a significant accessory phase with many overlapping reflections, we believe that a meaningful anisotropic refinement is not possible with this data set.

Inspection of the crystal structure at 4.2 K revealed an unexpected conformation for both of the symmetry-independent methanol molecules. The ideal methanol molecule, with point-group symmetry m (C_S), has D—C—O—D torsion angles of 180, 60 and 60°; whilst this perfect symmetry may not be preserved in solid-state structures, the largest D—C—O—D torsion angle is usually close to 180°. In methanol hemiammoniate at 4.2 K, however, we discovered D—C—O—D torsion angles of 134.6 (4), 108.2 (5) and 12.0 (5)° in methanol-1, and 148.4 (4), 96.8 (5) and 27.3 (5)° in methanol-2. A refinement in which extremely hard bond-distance restraints (the restraint weighting term FACTR was set to 10 000) were used to enforce the ideal molecular geometry was clearly disfavoured by the data; the goodness-of-fit deteriorated considerably to $R_p = 4.22\%$ ($\chi^2 = 45.09$). As a check on the correctness of the structure solution, the structure that was freely refined from the 4.2 K backscattering data was fixed and used to fit the data collected in the 90° detector banks and the low-angle bank. Here, only scale factors, diffractometer constants (DIFC and DIFA), background coefficients, peak-profile coefficients and one absorption coefficient were refined for each bank. The atomic coordinates and isotropic displacement parameters (U_{iso}) refined from the backscattering data and the overall powder statistics for all three detector banks are reported in Table 1, along with selected inter-atomic bond lengths and angles. The latter will be discussed in the following section. The quality of the fit to the diffraction data is illustrated in Fig. 2. It is worth pointing out the consistency in the displacement parameters for the deuterons of the two symmetry-independent methanol molecules, which were not constrained in any way to be equal, and are also nearly identical to the equivalent U_{iso} values obtained from the anisotropic refinement of the methanol monoammoniate structure at 4.2 K (Fortes, Wood & Knight, 2009).

Application of the 4.2 K structural model to the 180 K backscattering 30–130 ms data set, refining only the unit-cell dimensions, U_{iso}, background and profile coefficients, resulted

Table 1
Refined structural parameters of methanol hemiammoniate at 4.2 K.

Powder statistics reported in italics refer to refinements in which the structural model obtained solely from the backscattering diffraction data was tested against data collected in the other two detector banks whilst keeping the structural parameters fixed.

		Fitted		Minus background	
Histogram	N_{data}	wR_p	R_p	wR_p	R_p
Backscattering	4337	2.23%	1.98%	2.82%	2.37%
90° banks	*1883*	*2.67%*	*2.07%*	*3.21%*	*2.35%*
Low-angle bank	*987*	*5.01%*	*3.62%*	*4.95%*	*3.69%*
Powder totals	*7207*	*2.65%*	*2.30%*	*3.21%*	*2.61%*
χ^2 (backscattering fit only) = 6.865 for 92 variables					

Unit-cell dimensions	*a*	*b*	*c*
	12.70615 (16) Å	8.84589 (9) Å	4.73876 (4) Å
Space group $Pn2_1a$, $Z = 4$		*V*	ρ_{calc}
		532.623 (8) Å^3	1149.57 (2) kg m^{-3}

Unit cell of co-existing methanol monoammoniate, present at 17.8 (2) wt%: a = 11.0386 (4), b = 7.6547 (3), c = 7.5847 (3) Å, V = 640.88 (3) Å^3.

Bond lengths and angles (Å, °) for the methanol molecules.

C1—D1	1.109 (5)	D1—C1—D2	107.6 (4)
C1—D2	1.089 (5)	D1—C1—D3	110.4 (4)
C1—D3	1.104 (5)	D2—C1—D3	106.6 (4)
C1—O1	1.408 (4)	O1—C1—D1	112.1 (4)
O1—D4	1.056 (5)	O1—C1—D2	110.8 (4)
		O1—C1—D3	109.2 (4)
		C1—O1—D4	108.0 (4)
		D4—O1—C1—D3	134.6 (4)
C2—D8	1.061 (5)	D8—C2—D9	109.5 (4)
C2—D9	1.093 (5)	D8—C2—D10	108.4 (4)
C2—D10	1.108 (5)	D9—C2—D10	105.4 (4)
C2—O2	1.421 (5)	O2—C2—D8	114.7 (3)
O2—D11	0.999 (5)	O2—C2—D9	110.2 (4)
		O2—C2—D10	108.2 (4)
		C2—O2—D11	105.7 (4)
		D11—O2—C2—D10	148.4 (4)

Bond lengths and angles (Å, °) for the ammonia molecule.

N1—D5	1.032 (4)	D5—N1—D6	103.5 (3)
N1—D6	1.033 (4)	D5—N1—D7	108.0 (4)
N1—D7	0.985 (4)	D6—N1—D7	109.7 (4)

Hydrogen bonds and non-bonded intermolecular contacts (Å, °).

D4···N1	1.670 (4)	O1—D4···N1	2.724 (5)	O1—D4···N1	174.9 (4)
D5···O2	2.058 (5)	N1—D5···O2	3.080 (4)	N1—D5···O2	169.8 (3)
D6···O1	2.083 (5)	N1—D6···O1	3.090 (5)	N1—D6···O1	164.2 (3)
D7···O2	2.068 (5)	N1—D7···O2	3.015 (4)	N1—D7···O2	160.7 (4)
D11···O1	1.726 (5)	O2—D11···O1	2.721 (5)	O2—D11···O1	173.8 (4)
C···C	3.754 (4)				
O···O	4.151 (6)				
N···N	4.739 (3)				

Table 2
Refined structural parameters of methanol hemiammoniate at 180 K.

		Fitted		Minus background	
Histogram	N_{data}	wR_p	R_p	wR_p	R_p
Backscattering (30–130 ms)	4303	1.76%	1.54%	3.10%	2.44%
Backscattering (100–200 ms)	1975	4.31%	4.04%	6.01%	5.42%
90° banks (30–130 ms)	1883	1.75%	1.20%	1.72%	1.28%
90° banks (100–200 ms)	843	2.99%	2.54%	3.60%	3.00%
Low-angle bank (30–130 ms)	1099	4.02%	3.11%	4.25%	3.29%
Powder totals	10101	1.81%	2.08%	2.04%	2.82%
χ^2 (including contribution from bond-length restraints) = 57.47 for 95 variables					

Unit-cell dimensions	*a*	*b*	*c*
	12.90413 (16) Å	8.96975 (8) Å	4.79198 (4) Å
Space group $Pn2_1a$, $Z = 4$		*V*	ρ_{calc}
		554.656 (7) Å^3	1103.90 (1) kg m^{-3}

Unit cell of co-existing methanol monoammoniate, present at 17.8 (2) wt%: a = 11.2096 (3), b = 7.7456 (2), c = 7.6781 (2) Å, V = 666.66 (2) Å^3.

Bond lengths and angles (Å, °) for the methanol molecules. Entries in bold refer to interatomic contacts that were subjected to restraints during the refinement process (see text for further details).

C1—D1/*b*	**1.078 (3)/1.079 (2)**	D1—C1—D2/*b*	**111.1 (3)/110.7 (2)**
C1—D2/*b*	**1.075 (3)/1.080 (2)**	D1—C1—D3/*b*	**110.6 (2)/110.8 (2)**
C1—D3/*b*	**1.080 (3)/1.078 (2)**	D2—C1—D3/*b*	**111.0 (3)/110.5 (2)**
C1—O1	**1.427 (2)**	O1—C1—D1/*b*	**108.8 (3)/108.2 (2)**
O1—D4	**0.982 (3)**	O1—C1—D2/*b*	**106.5 (3)/108.1 (2)**
		O1—C1—D3/*b*	**108.6 (3)/108.4 (2)**
		C1—O1—D4	110.0 (3)
		D4—O1—C1—D3/D2*b*	136.9 (4)/163.8 (6)
C2—D8/*b*	**1.060 (3)/1.083 (2)**	D8—C2—D9/*b*	**110.2 (3)/110.2 (2)**
C2—D9/*b*	**1.104 (3)/1.078 (2)**	D8—C2—D10/*b*	**112.6 (3)/110.4 (2)**
C2—D10/*b*	**1.074 (3)/1.079 (2)**	D9—C2—D10/*b*	**109.2 (3)/110.9 (2)**
C2—O2	**1.423 (2)**	O2—C2—D8/*b*	**110.2 (3)/108.0 (2)**
O2—D11	**0.990 (3)**	O2—C2—D9/*b*	**105.7 (3)/108.8 (2)**
		O2—C2—D10/*b*	**108.7 (3)/108.5 (2)**
		C2—O2—D11	111.3 (3)
		D11—O2—C2—D10/D10*b*	158 (1)/138 (1)

Bond lengths and angles (Å, °) for the ammonia molecule. Entries in bold refer to interatomic contacts that were subjected to restraints during the refinement process (see text for further details).

N1—D5	**1.003 (2)**	D5—N1—D6	**109.6 (2)**
N1—D6	**1.006 (2)**	D5—N1—D7	**108.9 (2)**
N1—D7	**1.004 (2)**	D6—N1—D7	**109.4 (2)**

Hydrogen bonds and non-bonded intermolecular contacts (Å, °).

D4···N1	1.770 (4)	O1—D4···N1	2.748 (5)	O1—D4···N1	173.8 (4)
D5···O2	2.154 (4)	N1—D5···O2	3.153 (4)	N1—D5···O2	173.4 (3)
D6···O1	2.165 (4)	N1—D6···O1	3.143 (4)	N1—D6···O1	163.6 (3)
D7···O2	2.165 (4)	N1—D7···O2	3.127 (4)	N1—D7···O2	160.0 (3)
D11···O1	1.740 (5)	O2—D11···O1	2.716 (15)	O2—D11···O1	168.0 (4)
C···C	3.865 (4)				
O···O	4.261 (16)				
N···N	4.792 (3)				

in a tolerably good fit (R_p = 2.19%), and subsequent refinement of the atomic coordinates (using the bond-distance restraints) improved R_p to 1.88%. However, when this model was tested against the longer d-spacing data, in particular the 100–200 ms backscattering pattern and the 30–130 ms 90° diffraction pattern, some significant misfits became apparent. The most serious misfit, indicated in Fig. 3, relates to the 230 reflection from methanol hemiammoniate. This is of interest

because the methyl group of the 'bridging' methanol molecule (D1, D2 and D3) lies parallel to the 230 family of planes (d spacing = 2.7128 Å, see §3). (The other set of methyl deuterons lie in the 407 plane, at a d spacing of 0.6697 Å, which is not visible in any of the data we collected.) It is therefore likely that disorder in the methyl groups, upon warming to high homologous temperature, will give rise to large changes in the structure factor for these reflections. A difference Fourier map was synthesized from the complete 180 K data set, and examined for residual nuclear scattering density. Although the Fourier maps were noisy, positive features were located between the methyl deuterons of both methanol molecules. This result suggested to us that the methyl groups either are freely rotating or are hopping between two distinct orientations at 180 K. We chose to model two methyl group orientations, inserting a second trio of deuterons between the first, offset by a rotation about the C—O axis of 60°. Using all five 180 K diffraction patterns, and beginning with highly damped shifts, the occupancy of the methyl deuteron sites (constrained to sum = 1), the U_{iso} values and the atomic coordinates of the methyl deuterons were refined, subject to stiff bond-distance restraints. Ultimately, the complete structure was refined, the bond-distance restraints were relaxed (although not turned off) and the damping was reduced, until the refinement converged. As shown in Fig. 4 and reported in Table 2, this eliminated much of the residual misfit to the data and resulted in site occupancies for the two methyl orientations of ∼61:39 for methanol-1 and 52:48 for methanol-2. This refinement of a two-phase mixture, varying almost 100 structural parameters, probably represents the limits of the powder method, and a single-crystal analysis is essential to understand further the structural details of this crystal as a function of temperature.

3. Crystal structure of $CD_3OD{\cdot}0.5ND_3$

The atomic coordinates and isotropic displacement parameters are reported in the deposited CIF.[2] Inter- and intramolecular bond lengths and angles at 4.2 and 180 K are reported in Tables 1 and 2, respectively. Where these distances and angles have been subjected to restraints during the final cycle of refinement (albeit with a comparatively low weighting), they are reported in bold.

As shown in Fig. 5, the ND_3 molecule is tetrahedrally coordinated by the hydrophilic hydroxy moiety of the CD_3OD molecule. It accepts one O—D···N hydrogen bond of length 1.670 (4) Å at 4.2 K, and donates three N—D···O hydrogen bonds with lengths between 2.058 (5) and 2.083 (3) Å, both of these hydrogen-bond types being shorter than the equivalent bonds in methanol monoammoniate at the same temperature (1.746 Å and 2.152–2.256 Å, respectively). The O—D···N and O—D···O contacts are nearly linear (174–175°), but the N—D···O contacts are more bent, the angles ranging from 160.7 (4) to 169.8 (3)°; nonetheless, this bond angle is similar to that observed in the N—D···N bonds of solid ammonia [160.0 (2)°]. The hydrogen-bond lengths are typical for these donors and acceptors. The hydrogen-bonded ammonia–hydroxy chain structure (N1—D5···O2···D7—N1) extends along the c axis, being cross-linked along the a axis by the second hydroxy group (N1—D6···O1···D11—O2) to create a sheet in the ac plane (Fig. 6). The complete structure is built by donation of O1—D4···N1 hydrogen bonds directed approximately parallel to the b axis, joining adjacent sheets to form a fully three-dimensional hydrogen-bonded crystal. This structure contains broad eight-sided channels running along both the b and the c axes, within which sit the methyl groups of both symmetry-independent methanol molecules (Fig. 6c).

Unlike methanol monoammoniate, it appears that none of the methyl deuterons is involved in donation of a C—D···X hydrogen bond. In all instances, the shortest plausible methyl D···N or D···O distances are greater than the sums of the van der Waals radii of oxygen and hydrogen (2.72 Å) and nitrogen and hydrogen (2.75 Å) (Bondi, 1964), being in the range 2.78–3.09 Å. The two shortest contacts, D8···O1 = 2.781 (6) Å and D10···O2 = 2.890 (6) Å, are rather bent [C2—D8···O1 = 147.3 (4)° and C2—D10···O1 = 147.5 (4)°] and it seems most unlikely that these are even weakly hydrogen bonded. Clearly, the lack of hydrogen bonding reduces the size of the barrier to rotation of the methyl group. Our observations strongly suggest disorder of the methyl groups at high homologous temperatures over two distinct orientations (Fig. 7). Although we cannot preclude the possibility of dynamic disorder, we suggest that it is more likely to be static at this temperature; dynamic disorder might be expected to produce a substantial broad diffuse scattering signal, especially in the region of the 230 reflection, which is not obviously present.

4. Thermal expansion of $CD_3OD{\cdot}0.5ND_3$

Since data were collected at widely spaced temperatures, it is possible to obtain some information concerning the volu-

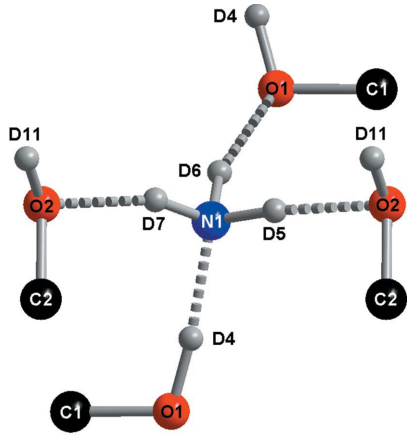

Figure 5
The tetrahedral coordination of the ammonia molecule by methanol in the crystal structure of methanol hemiammoniate. Atoms N1 and O2 comprise the zigzag chains in the structure, which are bridged across O1. The methyl deuterons have been omitted for clarity.

[2] Supplementary data for this paper are available from the IUCr electronic archives (Reference: DB5076). Services for accessing these data are described at the back of the journal.

metric and axial thermal expansion of methanol hemiammoniate. The relative volume change, $\Delta V/V$, upon warming from 4.2 to 180 K is +4.137%, which is comparable to the volume expansion found over a similar temperature range in other ammonia–methanol and water–methanol compounds, as well as solid methanol and solid ammonia, but it is much larger than in non-methanol-bearing compounds (see Table 4 in Fortes, Wood & Knight, 2009, and references therein). For example, the volume increase in methanol monoammoniate over the same temperature interval is +4.063%. In methanol hemiammoniate the expansion along each of the crystallographic axes is roughly similar ($\Delta a/a$ = 1.558%, $\Delta b/b$ = 1.400% and $\Delta c/c$ = 1.123%), indicative of comparatively isotropic thermo-elastic properties and supporting the observation of a fully three-dimensional hydrogen-bonded crystal. This contrasts with both methanol monohydrate and α-methanol, in which one crystallographic direction is dominated by weak van der Waals interactions instead of hydrogen bonds, resulting in a large thermal expansion along that direction, and thus a large anisotropy.

The O—D···N and N—D···O hydrogen bonds exhibit a comparatively small degree of expansion, in the range 4–6%, on warming from 4.2 to 180 K, whilst the O—D···O bond expands by only 0.8%.

Future powder diffraction measurements would be useful to determine with high precision the thermal expansivity up to the melting point, since the onset of methyl rotation/hopping on warming (or freezing-in of this motion on cooling) should be manifested in the unit-cell parameters. Single-crystal neutron diffraction measurements are necessary to understand the significant thermally induced structural changes in detail.

5. Summary

The crystal structure of perdeuterated methanol hemiammoniate has been determined from powder neutron diffraction data collected at 4.2 and 180 K. The crystal structure comprises a three-dimensional hydrogen-bonded network formed by zigzag chains of ND_3 and the OD group of one methanol molecule, cross-linked to one another by the OD group of the second methanol molecule to form sheets.

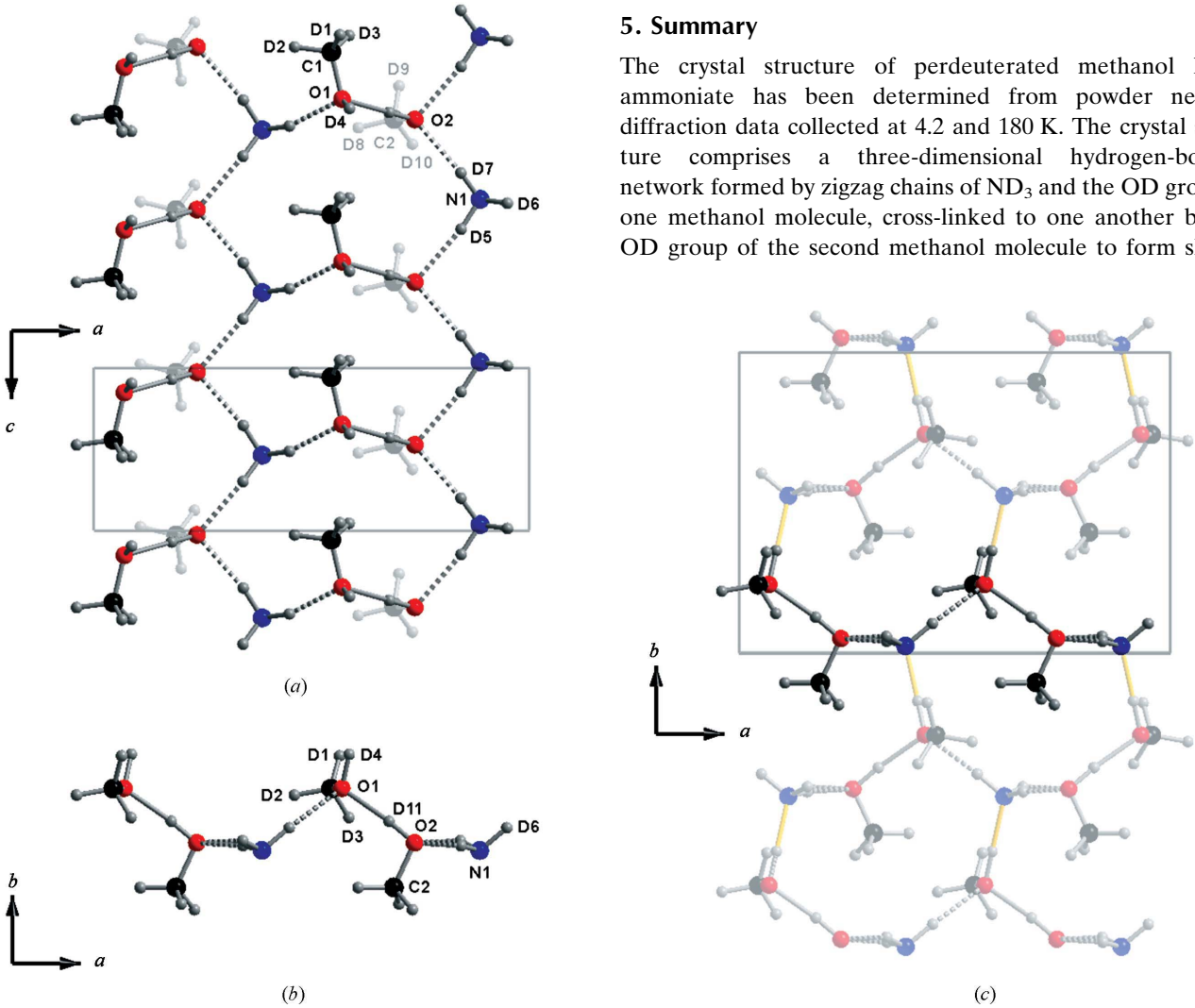

Figure 6
(*a*) The hydrogen-bonded ammonia–hydroxy chain structure (N1—D5···O2···D7—N1) in methanol hemiammoniate, extending along the *c* axis, illustrated perpendicular to the plane of the chain; the unit cell is outlined in grey. (*b*) The chains are bridged by the second hydroxy group (N1—D6···O1···D11—O2) to create a sheet in the *ac* plane. This sheet is viewed parallel to the *c* axis. (*c*) The complete structure is built by donation of O1—D4···N1 hydrogen bonds directed approximately parallel to the *b* axis, joining adjacent sheets to form a fully three-dimension hydrogen-bonded crystal. These bonds are marked in yellow. Notice the similarity of the open ring motif occupied by nonbonded methyl groups in both the *b*-axis and *c*-axis views (*a*) and (*c*). Atom labels correspond to those used in Tables 1 and 2.

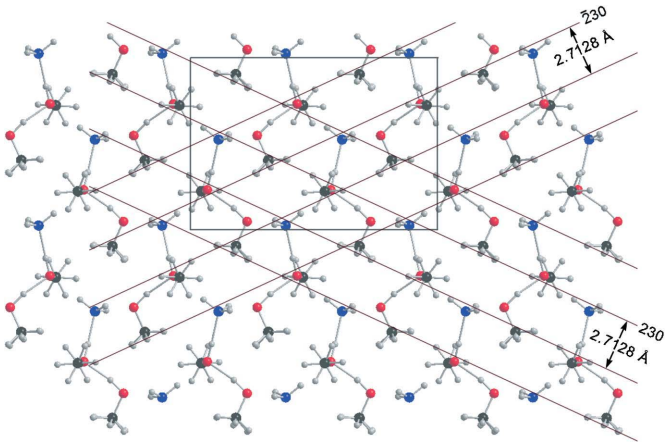

Figure 7
Illustration of the disordered model refined from the 180 K data, viewed along the *c* axis, with the *b* axis vertical and the *a* axis horizontal. A representative set of the 230 family of planes passing through the methyl groups (D1, D2, D3, and D1*b*, D2*b*, D3*b*) are shown. The outline of the unit cell is marked.

This second OD group donates hydrogen bonds to ammonia molecules in adjacent sheets. There is no evidence that the methyl groups are involved in hydrogen bonding, and there is good evidence to suggest that these groups are disordered at 180 K. The thermal expansion over the range 4.2–180 K is more nearly isotropic than is observed in methanol monohydrate, but very similar to what was observed previously in methanol monoammoniate.

This newly determined crystal structure contains a range of hydrogen-bond donors and acceptors of fundamental interest to physical chemists, and provides a natural laboratory for investigating these interactions.

The authors wish to thank the ISIS facility for beam time. We are also grateful to Dr Peter Grindrod for assistance during the experimental measurements. This work is supported by the Science and Technology Facilities Council, fellowship number PP/E006515/1.

References

Bondi, A. (1964). *J. Phys. Chem.* **68**, 441–451.
Boultif, A. & Louër, D. (2004). *J. Appl. Cryst.* **37**, 724–731.
Brink, G. & Glasser, L. (1982). *J. Comput. Chem.* **3**, 47–52.
Favre-Nicolin, V. & Černý, R. (2002). *J. Appl. Cryst.* **35**, 734–743.
Favre-Nicolin, V. & Černý, R. (2004). *Z. Kristallogr.* **219**, 847–856.
Feng, Y., Xie, R. & Wu, Z. (1999). *J. Chem. Eng. Data*, **44**, 401–404.
Finney, J. L. (1995). *Acta Cryst.* B**51**, 447–467.
Fortes, A. D. (2006). *Chem. Phys. Lett.* **431**, 283–288.
Fortes, A. D., Wood, I. G. & Brand, H. E. A. (2007). Experimental Report RB 610064. ISIS Facility, STFC Rutherford Appleton Laboratory, Chilton, Didcot, Oxfordshire, UK.
Fortes, A. D., Wood, I. G., Dobson, D. P. & Fewster, P. F. (2009). *Adv. Space Res.* **44**, 124–137.
Fortes, A. D., Wood, I. G. & Knight, K. S. (2009). *J. Appl. Cryst.* **42**, 1054–1061.
Frank, M. J. W., Kuipers, J. A. M. & van Swaaij, W. P. M. (1996). *J. Chem. Eng. Data*, **41**, 297–302.
Fraser, G. T., Suenram, R. D., Lovas, F. J. & Stevens, W. J. (1988). *Chem. Phys.* **125**, 31–43.
Hewat, A. W. & Riekel, C. (1979). *Acta Cryst.* A**35**, 569–571.
Hussein, M. A. & Millen, D. J. (1974). *J. Chem. Soc. Faraday Trans. 2*, **70**, 685–692.
Ibberson, R. M., David, W. I. F. & Knight, K. S. (1992). *The High Resolution Neutron Powder Diffractometer (HRPD) at ISIS – A User Guide.* Report RAL-92-031. Rutherford Appleton Laboratory, Chilton, Didcot, Oxfordshire, UK.
Inomata, H., Ikawa, N., Arai, K. & Saito, S. (1988). *J. Chem. Eng. Data*, **33**, 26–29.
Kanesaka, I. & Kawai, K. (1982). *Spectrochim. Acta A*, **38**, 549–554.
Kanesaka, I., Shozen, H. & Kawai, K. (1984). *Spectrochim. Acta A*, **40**, 383–386.
Kargel, J. S. (1990). PhD thesis, University of Arizona, Tucson, USA.
Kargel, J. S. (1992). *Icarus*, **100**, 556–574.
Larsen, A. C. & Von Dreele, R. B. (2000). *GSAS*. Report LAUR 86-748. Los Alamos National Laboratory, New Mexico, USA, http://www.ncnr.nist.gov/Xtal/software/gsas.html.
Li, Y., Liu, X., Wang, X. & Lou, N. (1997). *Chem. Phys. Lett.* **276**, 339–345.
Lopes, R. M. C. *et al.* (2007). *Icarus*, **186**, 395–412.
Loveday, J. S. & Nelmes, R. J. (2000). *Science and Technology of High Pressure: Proceedings of AIRAPT-17*, edited by M. H. Manghnani, W. J. Nellis & M. T. Nicol, pp. 133–136. Hyderabad: Universities Press.
Millen, D. J. & Zabicky, J. (1962). *Nature* (*London*), **196**, 889–890.
Millen, D. J. & Zabicky, J. (1965). *J. Chem. Soc.* **1965**, 3080–3085.
Schäfer, D., Xia, J., Vogt, M., Kamps, A. P.-S. & Maurer, G. (2007). *J. Chem. Eng. Data*, **52**, 1653–1659.
Smith, G. S. & Snyder, R. L. (1979). *J. Appl. Cryst.* **12**, 60–65.
Steiner, T. & Desiraju, G. R. (1998). *Chem. Commun.* pp. 891–892.
Toby, B. H. (2001). *J. Appl. Cryst.* **34**, 210–213.
Torrie, B. H., Binbrek, O. S., Strauss, M. & Swainson, I. P. (2002). *J. Solid State Chem.* **166**, 415–420.
Torrie, B. H., Weng, S.-X. & Powell, B. M. (1989). *Mol. Phys.* **67**, 575–581.
Wolff, P. M. de (1968). *J. Appl. Cryst.* **1**, 108–113.
Yukhnevich, G. V. & Tarakanova, E. G. (1998). *J. Mol. Struct.* **447**, 257–261.